

AN MME-BASED ATTITUDE ESTIMATOR USING VECTOR OBSERVATIONS

N95- 27775

John L. Crassidis
*Goddard Space Flight Center, Code 712
Greenbelt, MD 20771*

1995121354

F. Landis Markley
*Goddard Space Flight Center, Code 712
Greenbelt, MD 20771*

Abstract

In this paper, an optimal batch estimator and filter based on the Minimum Model Error (MME) approach is developed for three-axis stabilized spacecraft. Three different MME algorithms are developed. The first algorithm estimates the attitude of a spacecraft using rate measurements. The second algorithm estimates the attitude without using rate measurements. The absence of rate data may be a result of intentional design or from unexpected failure of existing gyros. The third algorithm determines input-torque modeling error trajectories. All of the algorithms developed in this paper use attitude sensors (e.g., three-axis magnetometers, sun sensors, star trackers, etc). Results using these new algorithms indicate that an MME-based approach accurately estimates the attitude, rate, and input torque trajectories of an actual spacecraft.

Introduction

The attitude of a spacecraft can be determined by either deterministic methods or by utilizing algorithms which combine dynamic models with sensor data. Three-axis deterministic methods, such as TRIAD [1], QUEST [2], and FOAM [3], require at least two simultaneous vector measurements to determine the attitude (direction-cosine) matrix. An advantage of both the QUEST and FOAM algorithms is that the attitude of a spacecraft can be estimated using more than two measurements. This is accomplished by minimizing a quadratic loss function first posed by Wahba [4]. However, all deterministic methods fail when only one vector measurement is available, (e.g., magnetometer data only). Estimation algorithms utilize dynamic models, and subsequently can (in theory) estimate the attitude of a spacecraft using measurements of a single reference vector. Although all spacecraft in use today have at least two on-board attitude sensors, estimation techniques can be used to determine the attitude during anomalous periods, such as solar eclipse and/or sensor co-alignment.

The most commonly used technique for attitude estimation is the Kalman filter [5]. The Kalman filter utilizes state-space representations to both estimate plant dynamics and also filter noisy data. Errors in the dynamical model and measurement process are assumed to be modeled by a zero-mean Gaussian process with known covariance. The optimality criterion in the Kalman filter minimizes the trace error covariance between estimated responses and model responses. In theory, the Kalman filter does not require actual measurements to satisfy this optimality criterion; however, in actual practice measurements are often used to properly "tune" the filter estimates.

Smoothing algorithms further refine state estimates by utilizing both a "forward filter" and a "backward filter" (see e.g., Gelb [6]). An advantage of smoothing algorithms is that the error covariance is always less or equal to either the forward or backward filter alone. A disadvantage of smoothing algorithms is that they cannot be implemented in sequential (real-time) estimation.

In order for the Kalman filter to be truly optimal, both the measurement error process and model error process must be random Gaussian processes with known covariance. In most circumstances,

properties of the measurement error process are known a priori by utilizing statistical inferences applied to sensor measurements. However, model error statistics are not usually well known. In actual practice the determination of the model error covariance in the Kalman filter is usually obtained by an ad hoc and/or heuristic approach, which can result in suboptimal filter designs (e.g., determining random gyro drift rate). Also, in many instances, such as nonlinear model errors or non-stationary processes, the assumption of a stationary Gaussian process can lead to severely degraded state estimates.

For spacecraft attitude estimation, the Kalman filter is most applicable to spacecraft equipped with three-axis gyros as well as attitude sensors [7]. However, rate gyros are generally expensive and are often prone to degradation or failure. Therefore, in recent years rate gyros have been omitted (e.g., in Small Explorer (SMEX) spacecraft, such as Solar Anomalous Magnetospheric Particle Explorer (SAMPEX) spacecraft). To circumvent the problem of rate gyro omission or failure, analytical models of rate motion can be used. This approach has been successfully used in a Real-Time Sequential Filter (RTSF) algorithm which propagates state estimates and error covariances using dynamic models [8]. The estimation of dynamic rates by the RTSF is accomplished from angular momentum model propagation, and then correcting for these rates by using a "gyro bias" component in the filter design. A clear advantage of using dynamic models is shown for the case of sun-magnetic field near co-alignment. For this case, deterministic algorithms, such as TRIAD and QUEST, show anomalous behaviors with extreme deviations in determined attitudes. Since the RTSF propagates an analytical model of motion, attitude estimates are improved even when data from only one attitude sensor is available. However, the RTSF is essentially a Kalman filter in which the "gyro bias" model (and subsequently the angular momentum model correction) is assumed to be a Gaussian process with known covariance. Also, fairly accurate models of angular momentum are required in order to obtain accurate estimates. Subsequently, the design process for choosing the model error covariance becomes difficult.

In this paper, an optimal attitude estimation algorithm is developed which is capable of robust and accurate state estimation for spacecraft lacking accurate or any rate measurements and/or accurate dynamic models. This algorithm is based on the Minimum Model Error (MME) [9] batch-estimation approach. The advantages of the MME estimator over conventional Kalman strategies include: (i) no a priori statistics on the form of the model error are required, (ii) the actual model error is determined as part of the solution, and (iii) state estimates are free of jump discontinuities, which greatly smoothes out high measurement noise. The MME estimation approach has been successfully applied to numerous poorly-modeled dynamic systems which exhibit highly nonlinear behaviors (see, e.g. [10-11]). Previous MME studies used TRIAD-determined quaternions as measurements [12]. The formulations developed in this paper expand upon this method to include attitude sensors, such as three-axis magnetometers (TAM), fine sun sensors (FSS), star trackers, etc.

The organization of this paper proceeds as follows. First, a summary of the spacecraft attitude kinematics and sensor models is shown. Then, a brief review of the MME estimator for nonlinear systems is shown. Next, various MME-based algorithms are developed for the purpose of attitude estimation, which include: a simple linear algorithm which is used to smooth noisy rate measurements, an attitude estimator using rate measurement information, an attitude estimator without the utilization of any rate measurements, and an input torque estimator. Finally, these MME designs are used to estimate the attitude, rate, and input torque trajectories of the SAMPEX spacecraft in order to demonstrate the usefulness of these algorithms.

Attitude Kinematics and Dynamics

In this section, a brief review of the kinematic and dynamic equations of motion for a three-axis stabilized spacecraft is shown. The attitude is assumed to be represented by a quaternion, defined as

$$\underline{q} \equiv \begin{bmatrix} q_1 \\ q_2 \\ q_3 \\ q_4 \end{bmatrix} \quad (1)$$

with

$$\underline{q}_{13} \equiv \begin{bmatrix} q_1 \\ q_2 \\ q_3 \end{bmatrix} = \hat{n} \sin(\theta / 2) \quad (2a)$$

$$q_4 = \cos(\theta / 2) \quad (2b)$$

where \hat{n} is a unit vector corresponding to the axis of rotation and θ is the angle of rotation. The quaternion kinematic equations of motion are derived by using the spacecraft's angular velocity ($\underline{\omega}$), given by

$$\dot{\underline{q}} = \frac{1}{2} \Omega(\underline{\omega}) \underline{q} = \frac{1}{2} \Xi(\underline{q}) \underline{\omega} \quad (3)$$

where $\Omega(\underline{\omega})$ and $\Xi(\underline{q})$ are defined as

$$\Omega(\underline{\omega}) \equiv \begin{bmatrix} -[\underline{\omega} \times] & \vdots & \underline{\omega} \\ \dots & \vdots & \dots \\ -\underline{\omega}^T & \vdots & 0 \end{bmatrix} \quad (4a)$$

$$\Xi(\underline{q}) \equiv \begin{bmatrix} q_4 I_{3 \times 3} + [\underline{q}_{13} \times] \\ \dots \\ -\underline{q}_{13}^T \end{bmatrix} \quad (4b)$$

The 3×3 dimensional matrices $[\underline{\omega} \times]$ and $[\underline{q}_{13} \times]$ are referred to as cross product matrices since $\underline{a} \times \underline{b} = [\underline{a} \times] \underline{b}$, with

$$[\underline{a} \times] \equiv \begin{bmatrix} 0 & -a_3 & a_2 \\ a_3 & 0 & -a_1 \\ -a_2 & a_1 & 0 \end{bmatrix} \quad (5)$$

Since a three degree-of-freedom attitude system is represented by a four-dimensional vector, the quaternions cannot be independent. This condition leads to the following normalization constraint

$$\underline{q}^T \underline{q} = q_{13}^T q_{13} + q_4^2 = 1 \quad (6)$$

Also, the matrix $\Xi(\underline{q})$ obeys the following helpful relations

$$\Xi^T(\underline{q}) \Xi(\underline{q}) = \underline{q}^T \underline{q} I_{3 \times 3} \quad (7a)$$

$$\Xi(\underline{q}) \Xi^T(\underline{q}) = \underline{q}^T \underline{q} I_{4 \times 4} - \underline{q} \underline{q}^T \quad (7b)$$

$$\Xi^T(\underline{q}) \underline{q} = \underline{0}_{3 \times 1} \quad (7c)$$

$$\Xi^T(\underline{q}) \underline{\lambda} = -\Xi^T(\underline{\lambda}) \underline{q} \text{ for any } \underline{\lambda}_{4 \times 1} \quad (7d)$$

The dynamic equations of motion, also known as Euler's equations, for a rotating spacecraft are given by ([13])

$$\dot{\underline{L}} = \underline{N} - \underline{\omega} \times \underline{L} = I_b \dot{\underline{\omega}} \quad (8)$$

where \underline{L} is the total angular momentum, \underline{N} is the total external torque (which includes, e.g., control torques, aerodynamic drag torques, solar pressure torques, etc.), and I_b is the inertia matrix of the spacecraft. If reaction or momentum wheels are used on the spacecraft, the total angular momentum is given by

$$\underline{L} = I_b \underline{\omega} + \underline{h} \quad (9)$$

where \underline{h} is the total angular momentum due to the wheels. Thus, Equation (8) can be re-written as

$$\dot{\underline{L}} = \underline{N} - \left[I_b^{-1} (\underline{L} - \underline{h}) \right] \times \underline{L} \quad (10)$$

The measurement model is assumed to be of the form given by

$$\underline{B}_B = A(\underline{q}) \underline{B}_I \quad (11)$$

where \underline{B}_I is a 3×1 dimensional vector of some reference object (e.g., a vector to the sun or to a star, or the Earth's magnetic field vector) in a reference coordinate system, \underline{B}_B is a 3×1 dimensional vector defining the components of the corresponding reference vector measured in the spacecraft body frame, and $A(\underline{q})$ is given by

$$A(\underline{q}) = \left(q_4^2 - \underline{q}_{13}^T \underline{q}_{13} \right) I_{3 \times 3} + 2 \underline{q}_{13} \underline{q}_{13}^T - 2 q_4 \left[\underline{q}_{13} \times \right] \quad (12)$$

which is the 3×3 dimensional (orthogonal) attitude matrix.

Minimum Model Error Estimation

In this section, a brief review of the Minimum Model Error (MME) estimation algorithm is shown. The essential feature of this batch estimator is that actual model error trajectories are determined during the estimation process, unlike most filter/smoothen algorithms which assume that the model error is a stochastic process with known properties. The MME algorithm determines the correction added to the assumed model which yields an accurate representation of the system's behavior. This is accomplished by solving an optimality condition using an output residual constraint. Therefore, accurate state estimates can be determined without the use of precise system representations in the assumed model.

The MME algorithm assumes that the state estimates are given by a preliminary model and a to-be-determined model error vector, given by

$$\hat{\underline{x}}(t) = \underline{f}[\hat{\underline{x}}(t), \underline{u}(t), \underline{d}(t), t] \quad (13a)$$

$$\hat{\underline{y}}(t) = \underline{g}[\hat{\underline{x}}(t), t] \quad (13b)$$

where \underline{f} is an $n \times 1$ model vector, $\hat{\underline{x}}(t)$ is an $n \times 1$ state estimate vector, $\underline{u}(t)$ is a $p \times 1$ vector of known inputs, and $\underline{d}(t)$ is an $n \times 1$ model error vector, \underline{g} is a $q \times 1$ measurement (sensitivity) vector, and $\hat{\underline{y}}(t)$ is a $q \times 1$ estimated output vector. State-observable discrete measurements are assumed for Equation (13b) in the following form

$$\tilde{\underline{y}}(t_k) = \underline{g}_k[\underline{x}(t_k), t_k] + \underline{v}_k \quad (14)$$

where $\tilde{\underline{y}}(t_k)$ is a $q \times 1$ measurement vector at time t_k , and \underline{v}_k is a $q \times 1$ measurement noise vector which is assumed to be a zero-mean, Gaussian distributed process with known covariance.

In the MME algorithm, the optimal state estimates are determined on the basis that the measurement-minus-estimate error covariance matrix must match the measurement-minus-truth error covariance matrix. This condition is referred to as the ‘‘covariance constraint,’’ shown as

$$\left\{ \tilde{\underline{y}}(t_k) - \underline{g}_k[\hat{\underline{x}}(t_k), t_k] \right\} \left\{ \tilde{\underline{y}}(t_k) - \underline{g}_k[\hat{\underline{x}}(t_k), t_k] \right\}^T = R_k \quad (15)$$

where R_k is the element-by-element (known) measurement error covariance. However, problems may arise using Equation (15) which are attributed to ‘‘small sample’’ statistics [14]. Therefore, in the typical case where the measurement error process is stationary, the average covariance can be used, given by

$$\frac{1}{m} \sum_{k=1}^m \left\{ \tilde{\underline{y}}(t_k) - \underline{g}_k[\hat{\underline{x}}(t_k), t_k] \right\} \left\{ \tilde{\underline{y}}(t_k) - \underline{g}_k[\hat{\underline{x}}(t_k), t_k] \right\}^T \approx R \quad (16)$$

where m is the total number of measurements.

Next, the following cost function is minimized with respect to $\underline{d}(\tau)$

$$J = \frac{1}{2} \sum_{k=1}^m \left\{ \tilde{\underline{y}}(t_k) - \underline{g}_k[\hat{\underline{x}}(t_k), t_k] \right\}^T R^{-1} \left\{ \tilde{\underline{y}}(t_k) - \underline{g}_k[\hat{\underline{x}}(t_k), t_k] \right\} + \frac{1}{2} \int_{t_0}^{t_f} \underline{d}^T(\tau) W \underline{d}(\tau) d\tau \quad (17)$$

where W is an $n \times n$ positive-definite weighting matrix. The necessary conditions for the minimization of Equation (17) lead to the following two-point-boundary-value-problem (TPBVP) [9]

$$\dot{\hat{\underline{x}}}(t) = \underline{f}[\hat{\underline{x}}(t), \underline{u}(t), \underline{d}(t), t] \quad (18a)$$

$$\underline{d}(t) = -W^{-1} \left[\frac{\partial \underline{f}}{\partial \underline{d}} \right]^T \underline{\lambda}(t) \quad (18b)$$

$$\dot{\underline{\lambda}}(t) = - \left[\frac{\partial \underline{f}}{\partial \hat{\underline{x}}} \right]^T \underline{\lambda}(t) \quad (18c)$$

$$\underline{\lambda}(t_k^+) = \underline{\lambda}(t_k^-) + H^T(t_k) \left\{ \tilde{\underline{y}}(t_k) - \underline{g}_k[\hat{\underline{x}}(t_k), t_k] \right\} \quad (18d)$$

$$H(t_k) \equiv \left. \frac{\partial \underline{g}}{\partial \hat{\underline{x}}} \right|_{\hat{\underline{x}}(t_k), t_k} \quad (18e)$$

where $\underline{\lambda}(t)$ is an $n \times 1$ co-state vector which is updated at each measurement point using Equation (18d). The boundary conditions are selected such that either $\underline{\lambda}(t_0^-) = \underline{0}$ or $\hat{\underline{x}}(t_0)$ is specified at the initial time and either $\underline{\lambda}(t_f^+) = \underline{0}$ or $\hat{\underline{x}}(t_f)$ is specified at the final time.

The solution of the TPBVP for a given weighting matrix yields a state estimate time trajectory which can be used to determine a measurement residual covariance matrix. The covariance constraint is satisfied when the proper balance between model error and measurement residual has been achieved. If the measurement residual covariance is higher than the known measurement error covariance (R), then W should be decreased to less penalize the model error. Conversely, if the residual covariance is lower than the known covariance, then W should be increased so that less unmodeled dynamics are added to the assumed system model. The optimal weighting matrix is therefore obtained when the covariance constraint in Equation (16) is satisfied.

Gyro Noise Smoother

Gyros tend to be noisy and have an inherent drift. Also, gyros are usually sampled at a higher frequency than attitude sensors. In order to first filter the noise, a simple MME-based smoothing algorithm can first be applied. This algorithm minimizes

$$J_g = \frac{1}{2} \sum_{k=1}^m \{ \tilde{\underline{\omega}}_g(t_k) - \hat{\underline{\omega}}_g(t_k) \}^T R_g^{-1} \{ \tilde{\underline{\omega}}_g(t_k) - \hat{\underline{\omega}}_g(t_k) \} + \frac{1}{2} \int_{t_0}^{t_f} \underline{d}_g^T(\tau) W_g \underline{d}_g(\tau) d\tau \quad (19)$$

subject to

$$\underline{\hat{\omega}}_g(t) = \underline{d}_g(t), \quad \underline{\hat{\omega}}_g(t_0) = \underline{\hat{\omega}}_{g0} \quad (20)$$

where $\underline{\hat{\omega}}_g(t)$ is the estimated gyro output, and $\underline{d}_g(t)$ is the model error correction. Minimizing Equation (19) leads to the following TPBVP

$$\underline{\hat{\omega}}_g(t) = -W_g^{-1} \underline{\lambda}_g(t), \quad \underline{\hat{\omega}}_g(t_0) = \underline{\hat{\omega}}_{g0} \quad (21a)$$

$$\underline{\dot{\lambda}}_g = \underline{0} \quad (21b)$$

$$\underline{\lambda}_g(t_k^+) = \underline{\lambda}_g(t_k^-) + R_g^{-1} \{ \tilde{\underline{\omega}}_g(t_k) - \hat{\underline{\omega}}_g(t_k) \}, \quad \underline{\lambda}_g(t_f^-) = \underline{0} \quad (21c)$$

The solution of Equation (21) can be determined by using a steady-state Riccati transformation (see [15] for details). This transformation leads to the following

$$P_i = \sqrt{\frac{W_{g_i}}{R_{g_i} \Delta t}} \quad (22a)$$

$$\underline{\dot{h}}_i(t) = \left[\frac{P_i}{W_{g_i}} \right] \underline{h}_i(t) \quad (22b)$$

$$\underline{h}_i(t_k^-) = \underline{h}_i(t_k^+) - \frac{1}{R_{g_i}} \tilde{\underline{\omega}}_{g_i}(t_k), \quad \underline{h}_i(t_f^+) = \underline{0} \quad (22c)$$

$$\hat{\underline{\omega}}_{g_i}(t) = \left[\frac{P_i}{W_{g_i}} \right] \hat{\underline{\omega}}_{g_i}(t) - \left[\frac{1}{W_{g_i}} \right] h_i(t), \quad \hat{\underline{\omega}}_{g_i}(t_0) = \hat{\underline{\omega}}_{g_{i_0}} \quad (22d)$$

where the subscript (i) represents each gyro measurement set, and Δt is the sampling interval. For a given weighting and measurement covariance, the first step is to determine the steady-state Riccati solution in using Equation (22a). Then, the inhomogeneous Riccati trajectory is solved backwards in time using Equation (22b), with discrete jumps at each measurement point given by Equation (22c). Finally, the smoothed gyro estimates are determined using Equation (22d). An advantage of this algorithm is not only the inherent smoothing properties, but also that the gyro estimates are totally continuous. Therefore, the generally discrete gyro measurements can be replaced with the continuous gyro estimates given by Equation (22d).

Attitude Estimation Using Rate Measurements

The MME attitude angular velocity estimation formulation using rate measurements minimizes the following cost function

$$J = \frac{1}{2} \sum_{k=1}^m \left\{ \tilde{\underline{B}}_B - A(\hat{\underline{q}}) \underline{B}_I \right\}^T \Big|_{t_k} R^{-1} \left\{ \tilde{\underline{B}}_B - A(\hat{\underline{q}}) \underline{B}_I \right\} \Big|_{t_k} + \frac{1}{2} \int_{t_0}^{t_f} \underline{d}^T(\tau) W \underline{d}(\tau) d\tau \quad (23)$$

subject to

$$\dot{\hat{\underline{q}}}(t) = \frac{1}{2} \Omega \left[\tilde{\underline{\omega}}_g(t) + \underline{d}(t) \right] \hat{\underline{q}}(t), \quad \hat{\underline{q}}(t_0) = \hat{\underline{q}}_0 \quad (24)$$

where $\tilde{\underline{\omega}}_g(t)$ is the rate measurement vector, $\hat{\underline{q}}(t)$ is the estimated quaternion, and $\tilde{\underline{B}}_B$ and \underline{B}_I are the spacecraft body measurement and corresponding inertial field vector, respectively. The model error (\underline{d}) is a correction to the rate measurements. which forces the model responses to satisfy the covariance constraint in Equation (16).

The TPBVP given by Equation (18) can be written as

$$\dot{\hat{\underline{q}}}(t) = \frac{1}{2} \Omega \left[\tilde{\underline{\omega}}_g(t) + \underline{d}(t) \right] \hat{\underline{q}}(t), \quad \hat{\underline{q}}(t_0) = \hat{\underline{q}}_0 \quad (25a)$$

$$\underline{d}(t) + \frac{1}{2} W^{-1} \Xi^T(\hat{\underline{q}}) \underline{\lambda}(t) = 0 \quad (25b)$$

$$\dot{\underline{\lambda}}(t) = \frac{1}{2} \Omega \left[\tilde{\underline{\omega}}_g(t) + \underline{d}(t) \right] \underline{\lambda}(t) \quad (25c)$$

$$\underline{\lambda}(t_k^+) = \underline{\lambda}(t_k^-) + H^T \Big|_{t_k} R^{-1} \left\{ \tilde{\underline{B}}_B - A(\hat{\underline{q}}) \underline{B}_I \right\} \Big|_{t_k}, \quad \underline{\lambda}(t_f^+) = \underline{0} \quad (25d)$$

The sensitivity matrix H in Equation (25d) can be derived as

$$H = 2 \Xi^T(l) \quad (26)$$

where

$$\underline{l} = \Psi(\underline{\hat{q}}) \underline{B}_I \quad (27a)$$

$$\Psi(\underline{\hat{q}}) \equiv \begin{bmatrix} -\underline{\hat{q}}_4 I_{3 \times 3} + [\underline{\hat{q}}_{13} \times] \\ \dots\dots\dots \\ \underline{\hat{q}}_{13}^T \end{bmatrix} \quad (27b)$$

The extension to using multiple attitude sensors is accomplished by using a partitioned residual output and sensitivity matrix, given by

$$\begin{bmatrix} H_1^T & \dots & H_q^T \end{bmatrix} \begin{bmatrix} \{ \underline{\tilde{B}}_{B_1} - A(\underline{\hat{q}}) \underline{B}_{I_1} \} \\ \vdots \\ \{ \underline{\tilde{B}}_{B_q} - A(\underline{\hat{q}}) \underline{B}_{I_q} \} \end{bmatrix} \quad (28)$$

The co-state update in Equation (25d) shows a nonlinear relationship with respect to the quaternion estimate. However, this nonlinearity can be reduced to be a *linear* function if the quaternions obey normalization and each attitude sensor is assumed isotropic. This can be shown by deriving the co-state update using

$$\frac{1}{2r} \frac{\partial}{\partial \underline{\hat{q}}} \left\{ [\underline{\tilde{B}}_B - A(\underline{\hat{q}}) \underline{B}_I]^T [\underline{\tilde{B}}_B - A(\underline{\hat{q}}) \underline{B}_I] \right\} \quad (29)$$

where the measurement covariance is now assumed to be isotropic for each sensor (i.e., the measurement errors in each one of the axes are assumed equal). Therefore, $R = rI_{3 \times 3}$, which is a valid assumption for almost all attitude sensors. In order to determine the partial derivative in Equation (29), the following identities and definitions are used

$$E(\underline{B}_I) \equiv \begin{bmatrix} -[\underline{B}_I \times] & \vdots & -\underline{B}_I \\ \dots\dots & \vdots & \dots\dots \\ \underline{B}_I^T & \vdots & 0 \end{bmatrix} \quad (30a)$$

$$A(\underline{\hat{q}}) = -\Xi^T(\underline{\hat{q}}) \Psi(\underline{\hat{q}}) \quad (30b)$$

$$\Psi(\underline{\hat{q}}) \underline{B}_I = E(\underline{B}_I) \underline{\hat{q}} \quad (30c)$$

$$E(\underline{B}_I) E(\underline{B}_I) = -I_{4 \times 4} \underline{B}_I^T \underline{B}_I \quad (30d)$$

Equation (29) can now be re-written as

$$\frac{1}{2r} \frac{\partial}{\partial \underline{\hat{q}}} \left\{ \underline{\tilde{B}}_B^T \underline{B}_B - 2 \underline{\hat{q}}^T \Omega(\underline{\tilde{B}}_B) E(\underline{B}_I) \underline{\hat{q}} + I_{4 \times 4} (\underline{B}_I^T \underline{B}_I) (\underline{\hat{q}}^T \underline{\hat{q}})^2 \right\} \quad (31)$$

The partial derivative in Equation (31) is given by

$$\frac{2}{r} \left\{ \Omega(\underline{\tilde{B}}_B) E(\underline{B}_I) \underline{\hat{q}} + (\underline{B}_I^T \underline{B}_I) (\underline{\hat{q}}^T \underline{\hat{q}}) \underline{\hat{q}} \right\} \quad (32)$$

Hence, if the quaternions obey normalization the following identity is true

$$\left\{ \Omega(\tilde{\underline{B}}_B)E(\underline{B}_I)\hat{\underline{q}} + (\underline{B}_I^T \underline{B}_I)\hat{\underline{q}} \right\} = \Xi(h)\left\{ \tilde{\underline{B}}_B - A(\hat{\underline{q}})\underline{B}_I \right\} \quad (33)$$

Therefore, if the sensor measurements are isotropic, the co-state update in Equation (25d) is linear with respect to the quaternion estimate.

The TPBVP shown in Equations (25a)-(25d) can be solved by using gradient techniques. The basic gradient procedure is to first guess for the model error trajectory (\underline{d}). Then, integrate the quaternion states forward using Equation (25a) and co-states backward using Equation (25c) accounting for discrete jumps in Equation (25d). The next search direction is given by Equation (25b). This procedure is continued until convergence is achieved.

Attitude Estimation without Rate Measurements

In this section, the MME estimator is derived for spacecraft which lack any rate information. The formulation is based upon using Euler's equation for modeling the angular momentum. The MME problem for this case minimizes the following cost function

$$J = \frac{1}{2} \sum_{k=1}^m \left\{ \tilde{\underline{B}}_B - A(\hat{\underline{q}})\underline{B}_I \right\}^T \Big|_{t_k} R^{-1} \left\{ \tilde{\underline{B}}_B - A(\hat{\underline{q}})\underline{B}_I \right\} \Big|_{t_k} + \frac{1}{2} \int_{t_0}^{t_f} \underline{d}^T(\tau) W \underline{d}(\tau) d\tau \quad (34)$$

subject to

$$\begin{bmatrix} \dot{\hat{\underline{q}}}(t) \\ \dot{\hat{\underline{L}}}(t) \end{bmatrix} = \begin{bmatrix} \frac{1}{2}\Omega(\hat{\underline{\omega}}) & 0_{4 \times 3} \\ 0_{3 \times 4} & -[\hat{\underline{\omega}} \times] \end{bmatrix} \begin{bmatrix} \hat{\underline{q}}(t) \\ \hat{\underline{L}}(t) \end{bmatrix} + \begin{bmatrix} 0_{4 \times 3} \\ I_{3 \times 3} \end{bmatrix} \underline{N}(t) + \begin{bmatrix} 0_{4 \times 3} \\ I_{3 \times 3} \end{bmatrix} \underline{d}(t), \quad \begin{bmatrix} \hat{\underline{q}}(t_0) \\ \hat{\underline{L}}(t_0) \end{bmatrix} = \begin{bmatrix} \hat{\underline{q}}_0 \\ \hat{\underline{L}}_0 \end{bmatrix} \quad (35)$$

where

$$\hat{\underline{\omega}}(t) = I_b^{-1} \left\{ \hat{\underline{L}}(t) - \tilde{\underline{h}}(t) \right\} \quad (36)$$

where $\tilde{\underline{h}}$ is the measured angular momentum due to the wheels. Minimizing Equation (34) leads to the following TPBVP

$$\begin{bmatrix} \dot{\hat{\underline{q}}}(t) \\ \dot{\hat{\underline{L}}}(t) \end{bmatrix} = \begin{bmatrix} \frac{1}{2}\Omega(\hat{\underline{\omega}}) & 0_{4 \times 3} \\ 0_{3 \times 4} & -[\hat{\underline{\omega}} \times] \end{bmatrix} \begin{bmatrix} \hat{\underline{q}}(t) \\ \hat{\underline{L}}(t) \end{bmatrix} + \begin{bmatrix} 0_{4 \times 3} \\ I_{3 \times 3} \end{bmatrix} \underline{N}(t) + \begin{bmatrix} 0_{4 \times 3} \\ I_{3 \times 3} \end{bmatrix} \underline{d}(t), \quad \begin{bmatrix} \hat{\underline{q}}(t_0) \\ \hat{\underline{L}}(t_0) \end{bmatrix} = \begin{bmatrix} \hat{\underline{q}}_0 \\ \hat{\underline{L}}_0 \end{bmatrix} \quad (37a)$$

$$\underline{d}(t) + W^{-1} \underline{\lambda}_L(t) = \underline{0} \quad (37b)$$

$$\begin{bmatrix} \dot{\underline{\lambda}}_q(t) \\ \dot{\underline{\lambda}}_L(t) \end{bmatrix} = \begin{bmatrix} \frac{1}{2}\Omega(\hat{\underline{\omega}}) & \vdots & 0_{4 \times 3} \\ \dots & \dots & \dots \\ \frac{1}{2}I_b^{-1}\Xi^T(\hat{\underline{q}}) & \vdots & -[\hat{\underline{\omega}} \times] + I_b^{-1}[\underline{L} \times] \end{bmatrix} \begin{bmatrix} \underline{\lambda}_q(t) \\ \underline{\lambda}_L(t) \end{bmatrix}, \quad \underline{\lambda}_L(t_f) = \underline{0} \quad (37c)$$

with discrete jumps in the co-states given by

$$\underline{\lambda}_q(t_k^+) = \underline{\lambda}_q(t_k^-) + H^T \Big|_{t_k} R^{-1} \left\{ \underline{\tilde{B}}_B - A(\hat{q}) \underline{B}_I \right\} \Big|_{t_k}, \quad \underline{\lambda}_q(t_f^+) = \underline{0} \quad (38)$$

The TPBVP given by Equations (37) and (38) can be solved by using a simple gradient-based search technique.

Input Torque Estimation

In this section, the MME estimator is used to estimate model error torques using angular rate trajectories. These angular rate trajectories are assumed to be known (e.g., from finite differenced attitude estimates, or from angular rate estimates from an MME design or other estimator). First, a measured angular momentum vector is determined by

$$\underline{\tilde{L}} = I_b \underline{\omega} + \underline{\tilde{h}} \quad (39)$$

In general, the angular momentum measurements in Equation (39) will be noisy due to the angular velocity measurements of the wheel speed. However, this noise is inherently smoothed by the MME estimator. The MME problem for determining the errors in the torque input of Euler's equation minimizes the following cost function

$$J = \frac{1}{2} \sum_{k=1}^m \left\{ \underline{\tilde{L}} - \underline{\hat{L}} \right\}^T \Big|_{t_k} R^{-1} \left\{ \underline{\tilde{L}} - \underline{\hat{L}} \right\} \Big|_{t_k} + \frac{1}{2} \int_{t_0}^{t_f} \underline{d}^T(\tau) W \underline{d}(\tau) d\tau \quad (40)$$

subject to

$$\underline{\dot{\hat{L}}}(t) = -[\underline{\omega}(t) \times] \underline{\hat{L}}(t) + \underline{N}(t) + \underline{d}(t), \quad \underline{\hat{L}}(t_0) = \underline{\hat{L}}_0 \quad (41)$$

Minimizing Equation (40) leads to the following TPBVP

$$\underline{\dot{\hat{L}}}(t) = -[\underline{\omega}(t) \times] \underline{\hat{L}}(t) + \underline{N}(t) - W^{-1} \underline{\lambda}(t), \quad \underline{\hat{L}}(t_0) = \underline{\hat{L}}_0 \quad (42a)$$

$$\underline{\dot{\lambda}}(t) = -[\underline{\omega}(t) \times] \underline{\lambda}(t) \quad (42b)$$

$$\underline{\lambda}(t_k^+) = \underline{\lambda}(t_k^-) + R^{-1} \left\{ \underline{\tilde{L}} - \underline{\hat{L}} \right\}, \quad \underline{\lambda}(t_f^+) = \underline{0} \quad (42c)$$

The solution to the TPBVP in Equation (42) can be determined by using a Riccati transformation [15]. Applying this technique leads to the following equations

$$\dot{P}(t) = P(t)[\underline{\omega}(t) \times] + P(t)W^{-1}P(t) + [\underline{\omega}(t) \times]P(t) \quad (43a)$$

$$P(t_k^-) = P(t_k^+) + R^{-1}, \quad P(t_f^+) = 0 \quad (43b)$$

$$\underline{\dot{h}}(t) = \left\{ P(t)W^{-1} - [\underline{\omega}(t) \times] \right\} \underline{h}(t) - P(t)\underline{N}(t) \quad (43c)$$

$$\underline{h}(t_k^-) = \underline{h}(t_k^+) + R^{-1} \underline{\tilde{L}} \Big|_{t_k}, \quad \underline{h}(t_f^+) = \underline{0} \quad (43d)$$

$$\hat{\underline{L}}(t) = \left\{ -[\underline{\omega}(t) \times] - W^{-1} P(t) \right\} \hat{\underline{L}}(t) - W^{-1} \underline{h}(t) + \underline{N}(t), \quad \hat{\underline{L}}(t_0) = \underline{\hat{L}}_0 \quad (43e)$$

Therefore, the first step is to solve for the Riccati and inhomogeneous trajectories backwards in time using Equations (43a) and (43c), accounting for discrete jumps by Equations (43b) and (43d). Then, the angular momentum estimates are determined by integrating Equation (43e) forwards in time.

Attitude Estimation of an Actual Spacecraft

In this section, the MME estimation algorithms previously developed are used to estimate the attitude, rate, and input torque trajectories of the SAMPEX spacecraft using vector measurement observations. The SAMPEX general mission is to study energetic particles and various types of rays. The spacecraft is three-axis stabilized in a 550 by 675 km elliptical orbit with an 82° inclination. The attitude control hardware consists of a magnetic torquer assembly (MTA) and a reaction wheel assembly (RWA). The attitude determination hardware consists of five coarse Sun sensors (CSS) (primarily for Sun-acquisition), one fine Sun sensor (FSS), and a three-axis magnetometer (TAM). Also, no rate gyroscopic instruments are present on the spacecraft.

The onboard computer routine to determine attitude is based upon the TRIAD [1] deterministic method. The spacecraft is controlled by the MTA to maintain the fixed solar arrays perpendicular to the sun-line. The RWA is used to point the instrument boresight axis as required by the scientific mission. During eclipse no sun measurements are available from the FSS. Attitude control is maintained by using a constant sun-line vector as a “pseudo-measurement,” so that both the MTA and RWA are still utilized. During vector co-alignment, the spacecraft is placed in a “coast” mode in which the MTA is not used (see [16] for more details). The required nominal attitude determination accuracy is $\pm 2^\circ$. During anomalous conditions (eclipse and/or measurement vector co-alignment) the attitude cannot be determined by deterministic methods, such as TRIAD. The MME algorithms presented in this paper can determine the attitude using TAM measurements only, so that attitude accuracy may be checked for any deviations from nominal performance.

The inertial field trajectories are obtained by using a 8th order spherical harmonic model of the Earth’s magnetic field with International Geomagnetic Reference Field (IGRF) coefficients. Magnetometer measurements by the TAM are known to be extremely accurate (within 0.3 mG). However, experience has shown that errors in the magnetic field model have a standard deviation of about 3 mG [17]. Therefore, 9 mG² is chosen for the diagonal elements of the measurement covariance matrix.

The first test case involves using both TAM and FSS measurements. A plot of the finite differenced angular rates using TRIAD determined attitudes is shown in Figure 1. These rates are extremely noisy, which is due to the large digitization noise associated with the FSS measurements. The TRIAD determined rates are next used in the first MME formulation (with rate information), along with the TAM and FSS measurements. A plot of the MME estimated rates is shown in Figure 2. Clearly, these rates are smoother than the TRIAD determined rates. Next, the MME input torque estimator is applied using these estimated rates. A plot of the MME determined input torques is shown in Figure 3. These torques correspond to a correction to the dynamic model, so that the model responses match the vector measurement observations.

The second case involves using TAM measurements only to estimate the attitude and angular rates. The MME attitude estimator without rate measurements is used for this case. A plot of the estimated angular rate trajectories is shown in Figure 4. These angular rate estimates clearly show a rotation about the spacecraft’s y-axis, which is the desired motion. A plot of the error between the estimated MME attitudes and the attitudes determined by TRIAD is shown in Figure 5. A slight hangoff is seen in the pitch axis. This may be due to nonlinear effects in the magnetic field model (this hangoff is also seen in Kalman filter approaches for other spacecraft such as UARS). However, the MME algorithm is able to determine attitudes to within 0.3° using TAM data only. This can be useful in determining the attitude when deterministic methods fail.

Conclusions

In this paper, several MME algorithms were presented for use in attitude estimation using vector measurement observations. The first algorithm used angular rate measurements to determine attitude estimate trajectories. The second algorithm estimated the attitude trajectories without any rate measurement information. The third algorithm determined the required torque input trajectories so that the model responses match the vector observations. An advantage of all of these algorithms is that quaternion normalization was maintained, since linearization of the dynamic model was not needed. The MME-based algorithms were then applied to an actual spacecraft. Results indicated that an MME-based approach provides a robust algorithm which can be used to determine the attitude, rate, and modeling error torque trajectories of a spacecraft from vector measurements.

Acknowledgments

The first author's work is supported by a National Research Council Postdoctoral Fellowship tenured at NASA-Goddard Space Flight Center. The author greatly appreciates this support. Also, this author wishes to thank D. Joseph Mook for many the comments and suggestions made throughout this work.

References

- [1] Lerner, G.M., "Three-Axis Attitude Determination," *Spacecraft Attitude Determination and Control*, edited by J.R. Wertz, D. Reidel Publishing Co., Dordrecht, The Netherlands, 1978, pp. 420-428.
- [2] Shuster, M.D., and Oh, S.D., "Attitude Determination from Vector Observations," *Journal of Guidance and Control*, Vol. 4, No. 1, Jan.-Feb. 1981, pp. 70-77.
- [3] Markley, F.L., "Attitude Determination from Vector Observations: A Fast Optimal Matrix Algorithm," *The Journal of the Astronautical Sciences*, Vol. 41, No. 2, April-June 1993, pp. 261-280.
- [4] Wahba, G., "A Least-Squares Estimate of Satellite Attitude," Problem 65-1, *SIAM Review*, Vol. 7, No. 3, July 1965, pg. 409.
- [5] Kalman, R.E., "A New Approach to Linear Filtering and Prediction Problems," *Transactions of the ASME, Journal of Basic Engineering*, Vol. 82, March 1962, pp. 34-45.
- [6] Gelb, A., *Applied Optimal Estimation*, MIT Press, Cambridge, Mass., 1974.
- [7] Lefferts, E.J., Markley, F.L., and Shuster, M.D., "Kalman Filtering for Spacecraft Attitude Estimation," *Journal of Guidance, Control and Dynamics*, Vol. 5, No. 5, Sept.-Oct. 1982, pp. 417-429.
- [8] Challa, M.S., Natanson, G.A., Baker, D.E., and Deutschmann, J.K., "Advantages of Estimating Rate Corrections During Dynamic Propagation of Spacecraft Rates-Applications to Real-Time Attitude Determination of SAMPEX," *Proceedings of the Flight Mechanics/Estimation Theory Symposium*, NASA-Goddard Space Flight Center, Greenbelt, MD, 1994, pp. 481-495.
- [9] Mook, D.J., and Junkins, J.L., "Minimum Model Error Estimation for Poorly Modeled Dynamic Systems," *Journal of Guidance, Control and Dynamics*, Vol. 3, No. 4, Jan.-Feb. 1988, pp. 367-375.
- [10] Stry, G.I., and Mook, D.J., "An Analog Experimental Study of Nonlinear Identification," *Nonlinear Dynamics*, Vol. 3, No. 1, pp. 1-11.
- [11] McPartland, M.D., and Mook, D.J., "Nonlinear Model Identification of Electrically Stimulated Muscle," *Proceedings of the IFAC Symposium on Modeling and Control in Biomedical Engineering*, Galveston, TX, March 1994, pp. 23-24.
- [12] DePena, J., Crassidis, J.L., McPartland, M.D., Meyer, T.J., and Mook, D.J., "MME-Based Attitude Dynamics Identification and Estimation for SAMPEX," *Proceedings of the Flight Mechanics/Estimation Theory Symposium*, NASA-Goddard Space Flight Center, Greenbelt, MD, 1994, pp. 497-512.
- [13] Markley, F.L., "Equations of Motion," *Spacecraft Attitude Determination and Control*, edited by J.R. Wertz, D. Reidel Publishing Co., Dordrecht, The Netherlands, 1978, pp. 510-523.

- [14] Freund, J.E., and Walpole, R.E., *Mathematical Statistics*, Prentice-Hall Inc., Englewood, NJ, 1987.
- [15] Crassidis, J.L., Mason, P.A.C., and Mook, D.J., "Riccati Solution for the Minimum Model Error Algorithm," *Journal of Guidance, Control and Dynamics*, Vol. 16, No. 6, Nov.-Dec. 1993, pp. 1181-1183.
- [16] Flatley, T.W., Forden, J.K., Henretty, D.A., Lightsey, E.G., and Markley, F.L., "On-board Attitude Determination and Control for SAMPEX," *Proceedings of the Flight Mechanics/Estimation Theory Symposium*, NASA-Goddard Space Flight Center, Greenbelt, MD, 1990, pp. 379-398.
- [17] Challa, M.S., *Solar, Anomalous, and Magnetospheric Particle Explorer (SAMPEX) Real-Time Sequential Filter (RTSF)*, Evaluation Report, NASA-Goddard Space Flight Center, Greenbelt, MD, April 1993.

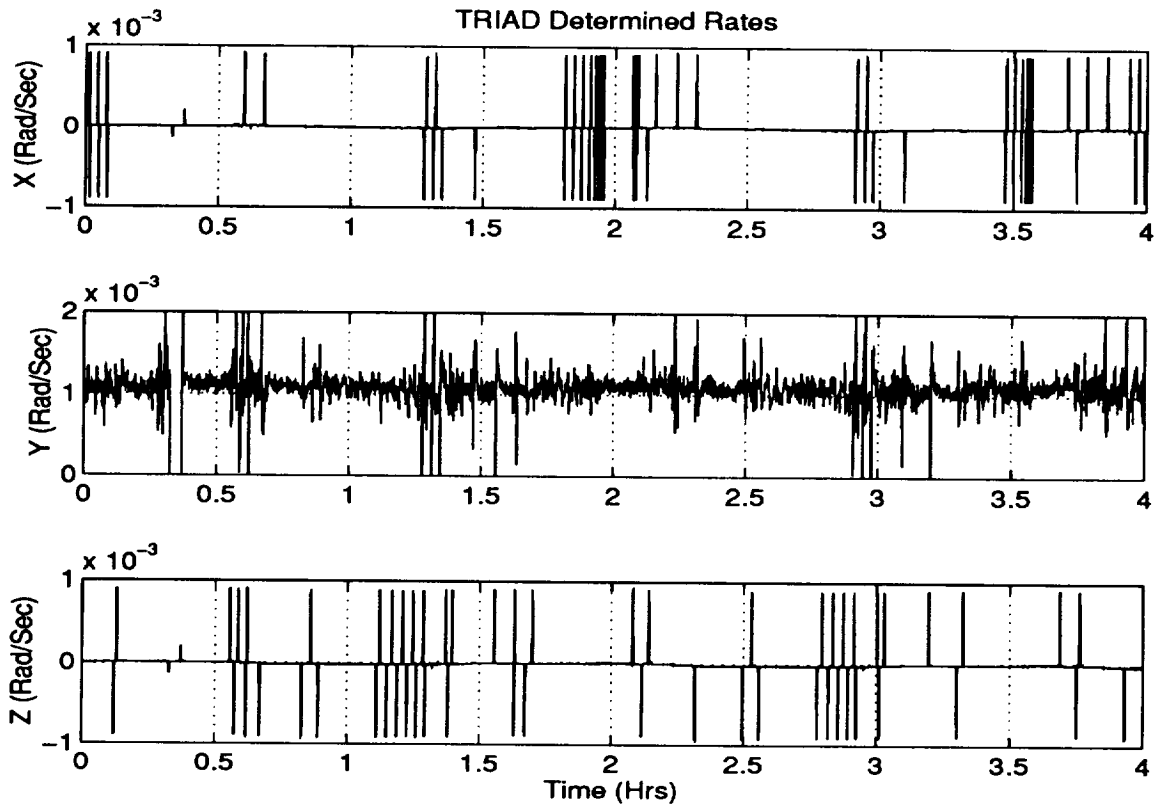


Figure 1 Plot of TRIAD Determined Attitude Rates

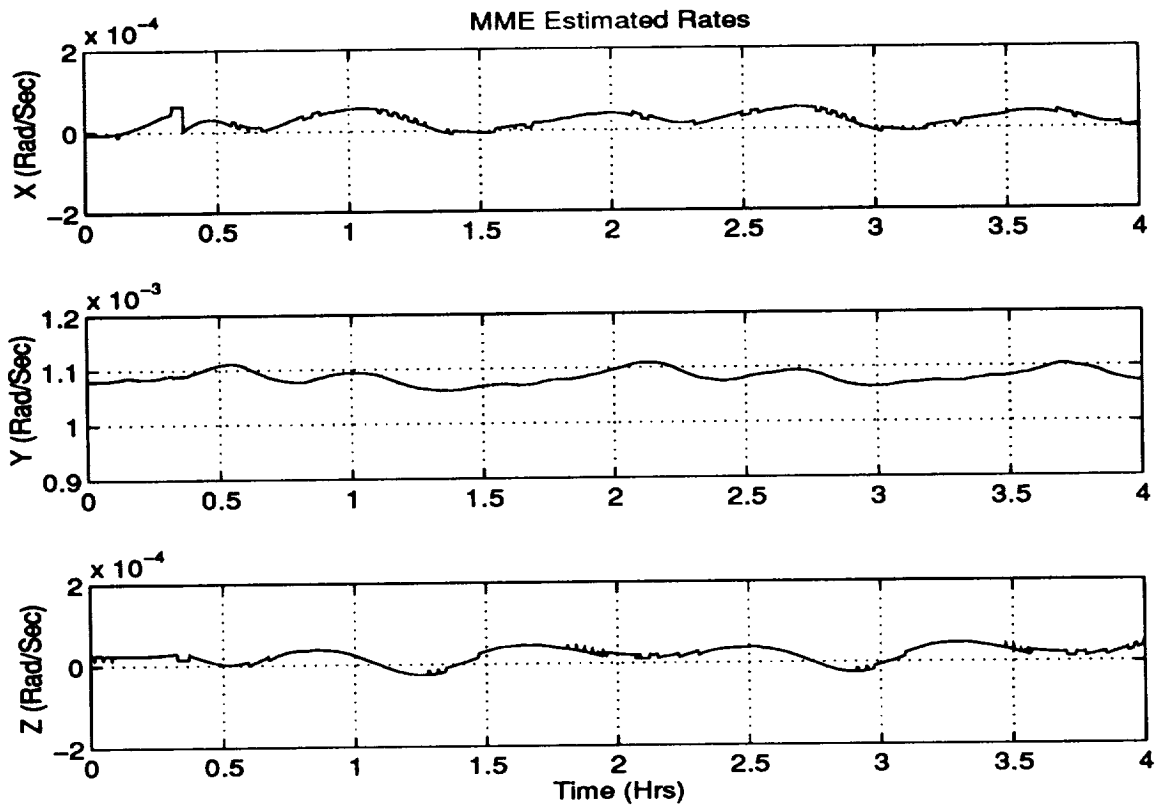


Figure 2 Plot of MME Estimated Rates

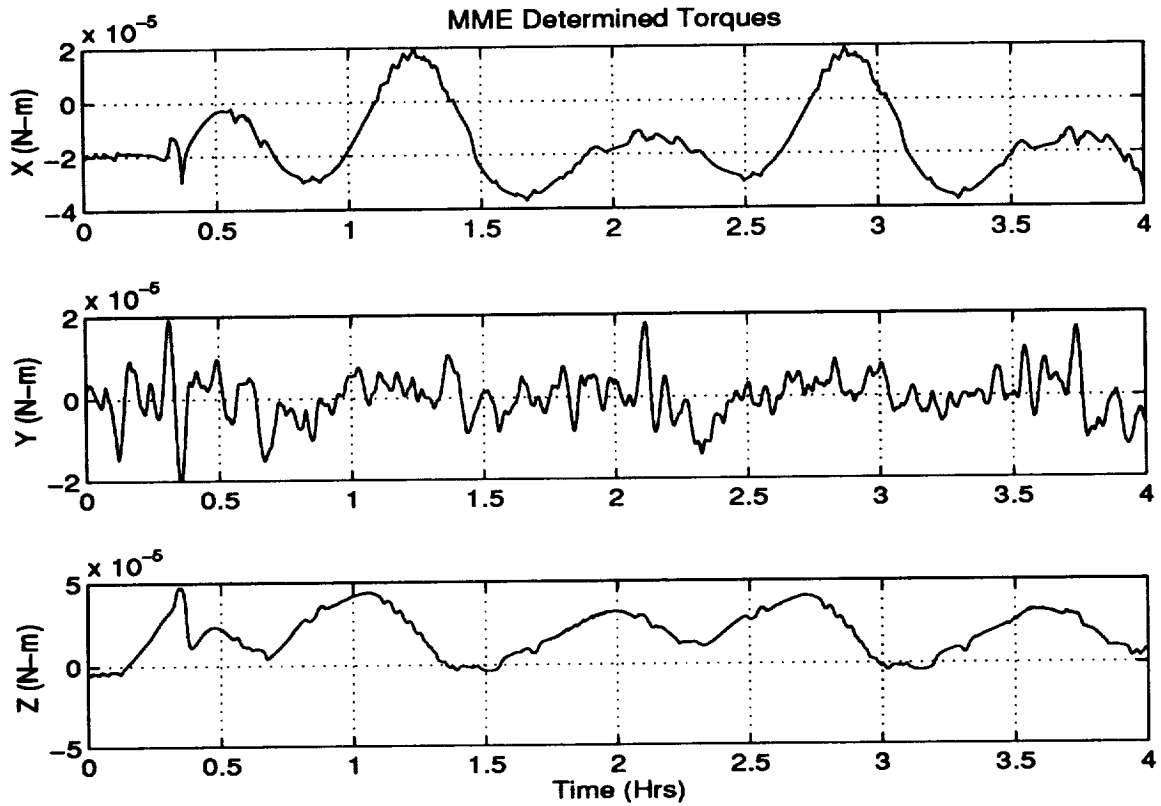


Figure 3 Plot of MME Determined Input Torques

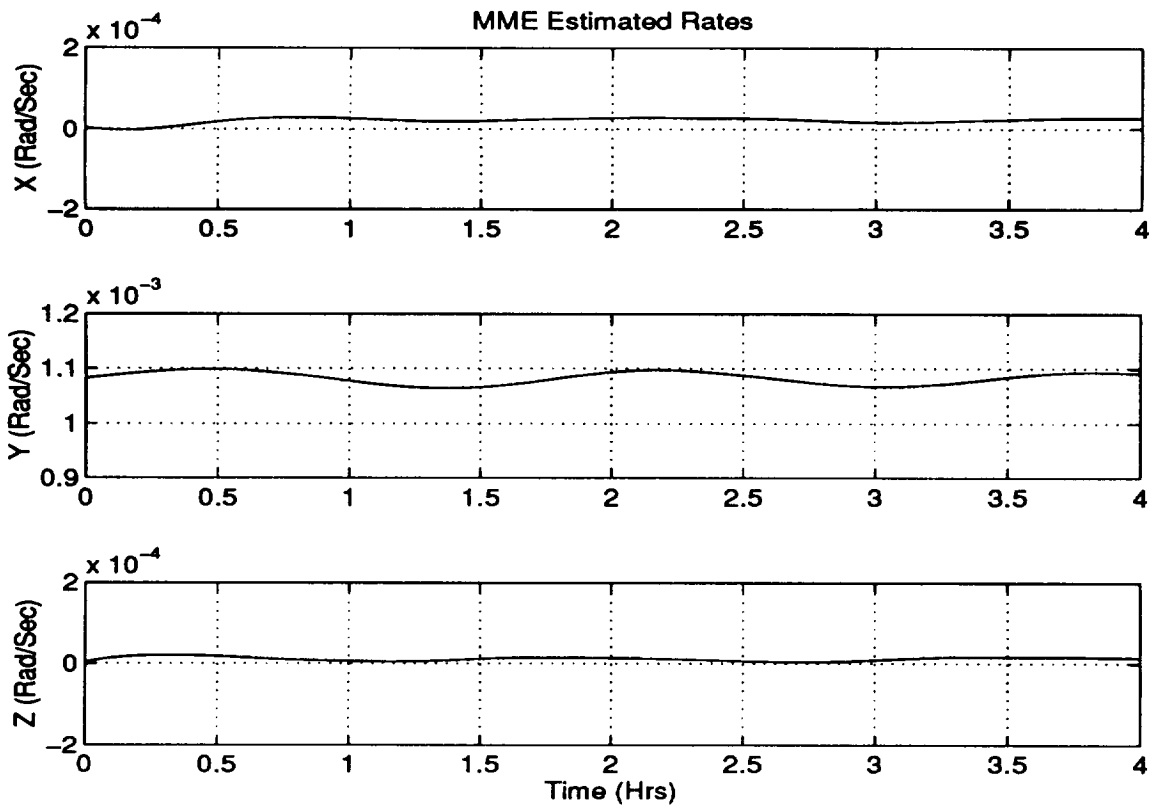


Figure 4 Plot of MME Estimated Rates Using TAM Data Only

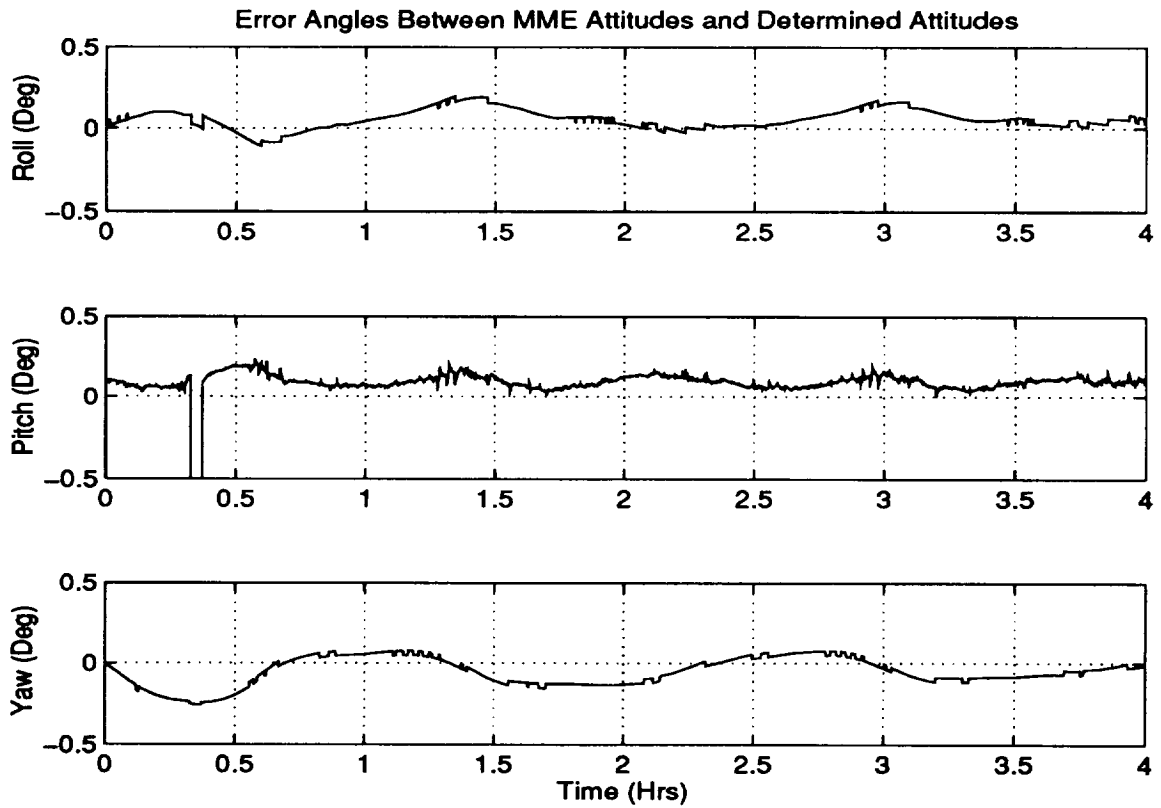


Figure 5 Plot of Attitude Errors Between TRIAD and MME

